ACS APPLIED MATERIALS & INTERFACES

Research Article

www.acsami.org

# Chemically Reduced Graphene Oxide for Ammonia Detection at Room Temperature

Ruma Ghosh,[†] Anupam Midya,[‡] Sumita Santra,[‡] Samit K. Ray,*[,‡] and Prasanta K. Guha*[,†]

[†]Department of Electronics & Electrical Communication Engineering and [‡]Department of Physics & Meteorology, IIT Kharagpur, Kharagpur, India 721302

Supporting Information

**ABSTRACT:** Chemically reduced graphene oxide (RGO) has recently attracted growing interest in the area of chemical sensors because of its high electrical conductivity and chemically active defect sites. This paper reports the synthesis of chemically reduced GO using $NaBH_4$ and its performance for ammonia detection at room temperature. The sensing layer was synthesized on a ceramic substrate containing platinum electrodes. The effect of the reduction time of graphene oxide (GO) was explored to optimize the response, recovery, and response time. The RGO film was characterized electrically and also with atomic force microscopy and X-ray photoelectron spectroscopy. The sensor response was found to lie between 5.5% at 200 ppm (parts per million) and 23% at 2800 ppm of ammonia, and also resistance recovered quickly without any application of heat (for lower concentrations of ammonia). The sensor was exposed to different vapors and found to be selective toward ammonia. We believe such chemically reduced GO could potentially be used to manufacture a new generation of low-power portable ammonia sensors.

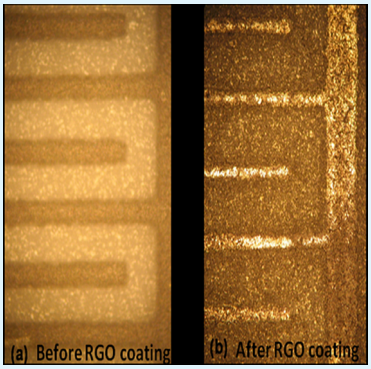


**KEYWORDS:** *ammonia sensor, room temperature ammonia detection, RGO synthesis, chemical reduction of GO, RGO-based sensor*

## INTRODUCTION

There has been increasing demand for the development of hand-held battery-operated reliable gas monitors for use in the automotive, environmental, and food industries and also for many niche areas.[1] These demands have led to the worldwide gas sensor research activity toward miniaturized low-power sensor development. In this respect, wide-band-gap metal oxide sensing material based solid-state gas sensors have been widely explored particularly because of their ability to respond to various toxic gases and volatile organic compounds (VOCs).[2−4] However, such materials sense analytes effectively at elevated temperatures, typically between 200 and 500 °C. Hence, metal oxide based gas sensors are usually power hungry (e.g., the commercially available Taguchi sensor consumes power between 200 mW and 1 W). Thus, one of the key research focuses nowadays is to develop gas sensors that will sense gases at room temperature (hence, much lower power consumption). In this regard, carbon nanomaterials, particularly graphene, are found to be very attractive. Graphene is a single flat atomic layer of carbon with atoms arranged in a two-dimensional honeycomb configuration.[5,6] There are several reasons for graphene to be highly sensitive toward different chemical analytes: (i) every carbon atom in graphene is a surface atom, which provides a very large surface-to-volume ratio, so that electron transport through graphene is highly sensitive to adsorbed molecular analytes; (ii) also it shows very high electrical conductivity.[7,8] Hence, graphene can be a potential competitor to metal oxides for the future new generation of microresistive gas sensors.

Ammonia is commonly found in industry and is a toxic gas that damages cells of the human body and causes injuries of the skin, eyes, and respiratory tract if exposed in large quantity (concentration > 300 ppm).[9,10] So, it is important to develop highly sensitive and selective ammonia sensors.

In this paper, we report the performance of a chemically reduced graphene oxide (RGO) on a ceramic substrate for ammonia detection at room temperature. The reduction time of graphene oxide (GO) was optimized to get better response, recovery, and response time, and its performance was explained for different durations of reduction. The response of the sensor was carried out in the presence of ammonia (200−2800 ppm) and different vapors.

## EXPERIMENTAL SECTION

**GO Synthesis.** We synthesized micrometer-sized water-soluble GO flakes from graphite powder using a modified Hummers and Offeman method.[11] For a detailed description, see the GO Synthesis section in the Supporting Information.

**GO Deposition and Reduction.** The basic substrate was made of platinum interdigitated electrodes (IDEs) deposited on a ceramic substrate (purchased from Synkera Technologies; part number Planar IDE Pt 0.25" P/N 610). The adjacent fingers of the IDEs are separated by a distance of 100 $\mu$m.

The IDEs were washed with an acetone and isopropyl alcohol solvent in an ultrasonic bath before dipping into an aqueous GO

Received: May 20, 2013
Accepted: July 15, 2013
Published: July 15, 2013

   dx.doi.org/10.1021/am4019109 | ACS Appl. Mater. Interfaces 2013, 5, 7599−7603

solution for 4 h. Then the GO-coated IDEs were dried in open air for 1 h. A 50 mM $NaBH_4$ solution was prepared by dissolving 19 mg of anhydrous $NaBH_4$ in 10 mL of water. The GO-coated IDEs were reduced using the hence-prepared $NaBH_4$ solution for 90 min. Because GO was dip-coated on the IDEs, the resulting film consisted of stacked layers of RGO. The average thickness of the RGO film was around 5 nm, which implies that the film was comprised of multilayered RGO.

GO is inherently insulating; however, the resistance of the device decreases significantly after reduction. RGO is a material that has higher electrical conductivity (compared to GO, where the side-chain oxygen functional group makes it electrically insulating) and chemically active defect sites, making it a potential candidate for gas sensing. There have been several reports of thermal reduction of GO films;[12−14] however, in this work, a chemical reduction approach was intentionally chosen to avoid any high-temperature process. Also, thermal reduction at low temperature usually makes the process time-consuming.[15−17] There have been several reports of reducing GO in chemical routes using hydrazine ($N_2H_4$).[18−20] However, hydrazine is toxic and often needs a long time (even 10 h or more) for the effective reduction of GO. Also, the C═N (hydrazone) group introduced during reduction remains in the sample.[21] It has also been reported that, in order to remove all of the oxygen functionalities of GO efficiently, hydrazine reduction has to be followed by heat treatment.[22] Shin et al. reported that the sheet resistance of GO reduced using $NaBH_4$ is lower than that of GO reduced using hydrazine.[23] Also, among the other substituted borohydrides, $NaBH_4$ is the most efficient reducing agent.[24] Hence, in this work, $NaBH_4$ was used as a reducing agent, which is nontoxic in nature and takes only 1−2 h to reduce GO.

**Material Characterizations and Gas Testing.** The sensing material was characterized using a probe station (electrical characterization), optical microscopy, atomic force microscopy (AFM), and X-ray photoelectron spectroscopy (XPS).

For gas testing, the sensor device was mounted in a stainless steel airtight chamber. The gas flow was controlled by an MKS mass flow controller, and the maximum flow rate was set to 100 sccm (standard cubic centimeters per minute). The resistance of the RGO film increases with an increase in the ammonia concentration; such a sensor is known as a resistive sensor. The gas chamber was connected to a custom-made test and measurement system interfaced with an Agilent 34972A LXI Data Acquisition Card so that the change in resistance of RGO in the presence of ammonia can be recorded automatically. The testing was carried out at room temperature. The sensors were first exposed to nitrogen ($N_2$) to stabilize the baseline resistance. Then the sensors were exposed to ammonia for 15 min and subsequently purged for 20 min in $N_2$. This step was repeated for six different concentrations of ammonia, varying from 200 to 2800 ppm.

## RESULTS AND DISCUSSION

The current−voltage ($I/V$) characteristics of the RGO film were measured using Keithley 4200 Semiconductor Characterization Systems and a probe station (Everbeing Int'l Corp.). The linear $I/V$ plot (shown in Figure 1) confirms good ohmic contact between the sensing material and the IDEs.

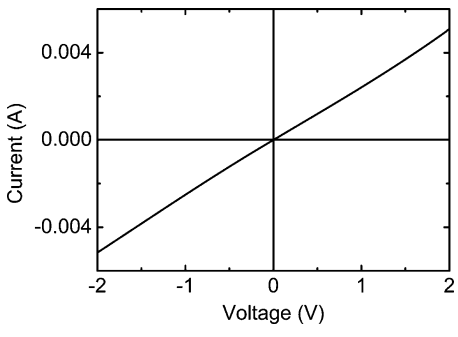


**Figure 1.** $I/V$ characteristics of the RGO-coated IDE.

The sensing material was also characterized using AFM (Veeco Nanoscope-IV). The dimensions and thickness of the GO sheets were evaluated by an AFM system. As shown in the AFM image in Figure 2, the dimensions of the GO flakes varied from ∼200 nm to ∼5 $\mu$m with a thickness of 2 nm (bilayer).

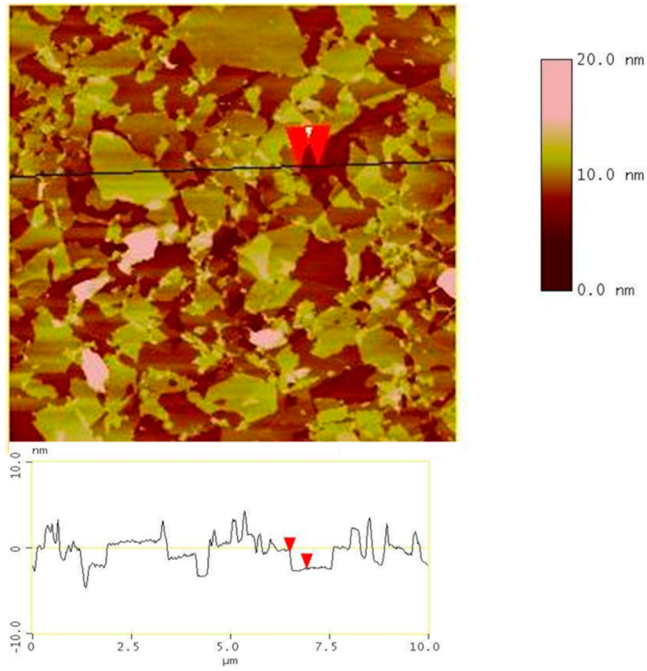


**Figure 2.** AFM image of GO with section analysis.

From gas testing, it was observed that the RGO resistance (and, hence, the response) increased with an increase in the ammonia concentration. The response was found to vary from 5.5% at 200 ppm to 23% at 2800 ppm ammonia, as shown in

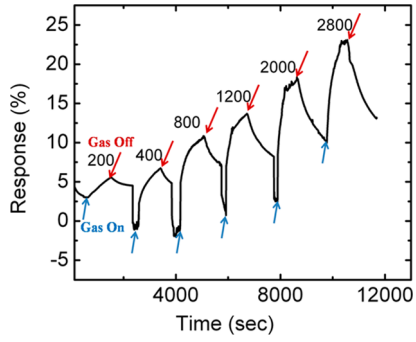


**Figure 3.** Response of a RGO-based sensor to $NH_3$ at six different concentrations (200−2800 ppm).

Figure 3. Here RGO was synthesized after reduction of GO for 90 min. The response of the sensor was calculated as

$$\frac{R_{\text{ammonia}} - R_{N_2}}{R_{N_2}} \times 100\% = \frac{\Delta R}{R_{N_2}} \times 100\%$$

where $R_{N_2}$ is the resistance of RGO in the presence of $N_2$ and $R_{\text{ammonia}}$ is the resistance of RGO in the presence of ammonia vapor. The response we got is much better than that in the recently reported works on ammonia sensing by carbon


dx.doi.org/10.1021/am4019109 | ACS Appl. Mater. Interfaces 2013, 5, 7599−7603

nanomaterials.[25,26] For example, Yu et al. in 2011 got a response of 13% ($R_{ammonia}/R_{air}$ = 1.13) with graphene sheets in the presence of 10000 ppm of ammonia, and Cui et al. in 2012 got a response of only 9% using silver-nanocrystal-functionalized carbon nanotubes in the presence of 10000 ppm of ammonia.

In the literature, it was reported by several groups that the thermal energy at room temperature is typically not enough to overcome the activation energy needed for molecular desorption, and hence high-temperature desorption is necessary for a full recovery. However, this heating will increase power consumption and also device complexity (a requirement of additional circuits). However, in our case, the sensors recovered (recovery time means the time required to reach 10% of the base resistance value) quickly without any application of heat especially after exposure at lower concentrations of ammonia. Recent works on graphene- and graphene-hybrid-based ammonia detectors with quick recovery and response at room temperature have also been reported.[27−30] Like Cui et al. synthesized, silver nanoparticles decorated RGO hybrids for ammonia detection. Their response plot shows a quick response and recovery of the sensor at room temperature for 10000 ppm of ammonia, but their response is much lower (only around 17%) than that of our device.[30]

The response of our device varied linearly with the gas concentration, as is shown in Figure 4.

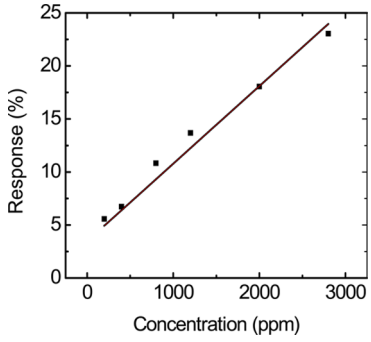


**Figure 4.** Linear fitted response versus concentration with a 90 min reduced sample (Adj $R^2$ = 0.98602).

To check the reproducibility of our device, sensing was carried out on four devices and the response was within 13% of the error range for all of the devices, as can be seen in Figure 5.

There have been some reports on the description of an ammonia-sensing mechanism by RGO.[31,32] RGO is intrinsically a p-type material,[33] and in the interaction between $NH_3$ and RGO, the former acts as a donor.

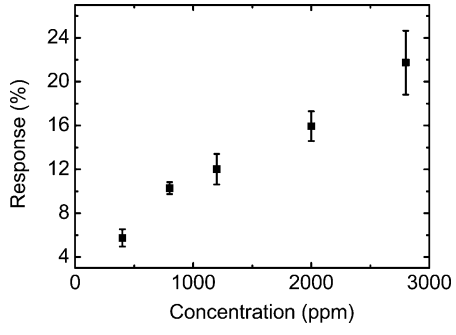


**Figure 5.** Response variation of four different devices at room temperature.

To gain insight into the mechanism of the gas-sensing property, sensing experiments were performed by employing RGO obtained after reducing GO for three different time periods on the same device. XPS measurements [PHI 5000 Versa Probe II (ULVAC-PHI Inc., Japan)] were performed to check the drop of the C−O group before and after the reduction of GO. From the narrow scan, areas under the C 1s region (C−O and C−C) were calculated. The ratio of C−O [binding energy (BE) = 286.3 eV] and C−C (BE = 284.6 eV) was found to be 1:1.01 in GO, and it decreased to 1:1.429, 1:1.86, and 1:2.2 in RGO after 30, 90, and 180 min of reduction, respectively, as shown in Figure 6.

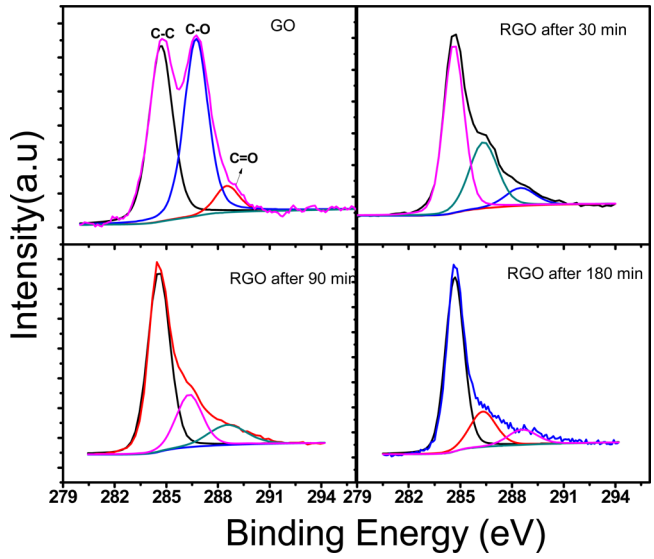


**Figure 6.** High-resolution XPS C 1s spectra of GO and RGO showing significant losses of C−O and C═O groups after 30, 90, and 180 min of reduction.

A $NH_3$ molecule gets physisorbed on the high surface area of pristine graphene. However, chemically derived RGO consists of defect sites and functional groups. So, the sensing mechanism includes physisorption as well as chemisorption of $NH_3$ mainly through hydrogen bonding at the defect sites and with the functional groups (carboxyl, carbonyl, epoxy, and hydroxyl).[34]

From gas testing, it was observed that the device with shorter reduction time (30 min) of GO senses ammonia with higher response than the longer reduction time of 180 min. This is because vigorous reduction (say, 180 min) with $NaBH_4$ generates RGO with less functionality and defects and more C═C $sp^2$-bonded carbon atoms; hence, molecular physisorption of $NH_3$ on RGO dominates, which gives rise to a lower response (as shown in Figure 7a). The recovery time of the 30 min reduced film (3505 s at 2800 ppm of $NH_3$) was longer than that of 90 min (1340 s at 2800 ppm of $NH_3$) and 180 min (1270 s at 2800 ppm of $NH_3$), as shown in Figure 7c. The epoxy and hydroxyl groups gradually get removed after reducing GO for a longer time, say 90 or 180 min. So, charge transfer between $NH_3$ and RGO majorly occurs at defect sites. Hence, more physisorption takes place than chemisorption, and the recovery is faster than that of 30 min reduced RGO. This implies that more defects and oxygen functionality mean more


dx.doi.org/10.1021/am4019109 | ACS Appl. Mater. Interfaces 2013, 5, 7599−7603

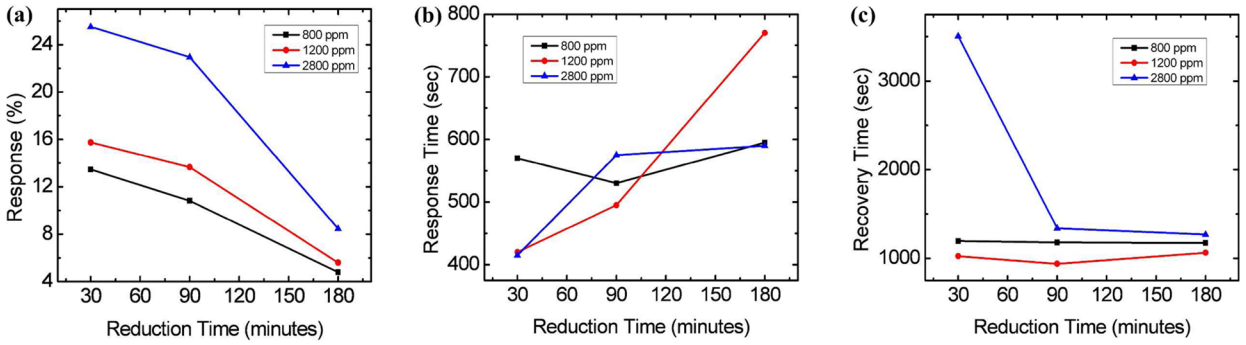


**Figure 7.** Comparative plots of devices after reducing GO for 30, 90, and 180 min at three different concentrations of ammonia (800, 1200, and 2800 ppm). (a) Response plot. (b) Response time plot. (c) Recovery time plot.

response; however, the recovery time decreases with an increase in the amount of $sp^2$-bonded atoms. This sensing mechanism is also in agreement with the works reported in the literature.[34−36] The 90 min reduced film shows a response close to that of the 30 min reduced film (as shown in Figure 7a), and also it (90 min) recovers as fast as 180 min reduced RGO. So, it can be concluded that a GO film with moderate reduction using $NaBH_4$ (for around 90 min) can give rise to a sensing layer that will possess defects, functional groups, and $sp^2$-bonded carbon atoms in a balanced amount, so that an optimum sensor performance was obtained from the point of view of the response, response time, and recovery time.

The selectivity of the RGO film was also studied by measuring the change in resistance of the sensing layer in the presence of several VOCs. In this regard, the device was exposed to 70 sccm of tetrahydrofuran (THF), acetone, chloroform, chlorobenzene, toluene, and methanol at room temperature (in our case, 70 sccm corresponds to 2800 ppm of ammonia). A comparative plot of the responses given by the sensor to these VOCs is shown in Figure 8. It was found that the RGO film showed excellent selectivity toward ammonia among various VOCs tested.

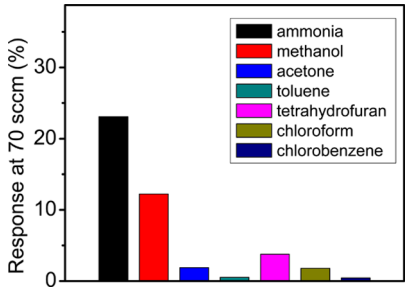


**Figure 8.** Comparative plots of all VOCs at 70 sccm.

Although we emphasized room temperature operation of our device, in order to discover the response of RGO-based gas sensors at higher temperature, sensing was also carried out at 50 and 100 °C. See Figure 1s in the Supporting Information.

## CONCLUSIONS

Chemically derived graphene-based gas sensors on ceramic substrates have been developed. The GO film was reduced for different time periods to see its effect on the ammonia response, response time, and recovery time. It was found that 90 min reduction is the optimized condition for highest response, recovery, and response time. RGO was found to be sensitive toward ammonia, and it showed moderately fast recovery even at room temperature. Different VOCs were also tested, but it was found that the sensing material is more selective toward ammonia. We believe such a low power, sensitive, and selective sensor will be useful for the development of a new generation of ammonia sensors.

## ASSOCIATED CONTENT

### Supporting Information

Details of GO synthesis and high-temperature (50 and 100 °C) measurement results. This material is available free of charge via the Internet at http://pubs.acs.org.

## AUTHOR INFORMATION

### Corresponding Author

*E-mail: pkguha@ece.iitkgp.ernet.in (P.K.G.), physkr@phy.iitkgp.ernet.in (S.K.R.). Phone: +91-3222-283538 (P.K.G.), +91-3222-283838 (S.K.R.). Fax: +91-3222-255303 (P.K.G.), +91-3222-255303 (S.K.R.).

### Author Contributions

R.G. designed and performed the research. A.M. assisted in the material synthesis and XPS and AFM characterization. S.S. cowrote the manuscript and assisted in gas sensor testing. S.K.R. provided guidance and manuscript preparation. P.K.G. provided overall guidance and wrote the manuscript. All authors discussed the results and have given approval to the final version of the manuscript.

### Notes

The authors declare no competing financial interest.

## ACKNOWLEDGMENTS

S.S. acknowledges the Department of Science and Technology (DST), India, for partial support of the work (Project SR/S2/RJN-104/2011). We also acknowledge the DST FIST Lab (in the Department of Physics & Meteorology) for use of the X-ray photoelectron spectrometer and the MEMS & Microelectronics Lab (in the Department of E&ECE) for use of the optical microscope of IIT Kharagpur.

## REFERENCES

(1) Gardner, J. W.; Guha, P. K.; Covington, J. A. *IEEE Sens. J.* **2010**, *10* (12), 1833−1848.

(2) Santra, S.; Guha, P. K.; Ali, S. Z.; Hiralal, P.; Unalan, H. E.; Covington, J. A.; Amaratunga, G. A. J.; Milne, W. I.; Gardner, J. W.; Udrea, F. *Sens. Actuators, B* **2010**, *146*, 559−565.

(3) Barsan, N.; Koziej, D.; Weimar, U. *Sens. Actutaors, B* **2007**, *121*, 18−35.

(4) Rahman, M. M.; Jamal, A.; Khan, S. B.; Faisal, M. *ACS Appl. Mater. Interfaces* **2011**, *3*, 1346−1351.
(5) Geim, A. K.; Novoselov, K. S. *Nat. Mater.* **2007**, *6*, 183−191.
(6) Dreyer, D. R.; Ruoff, R. S.; Bielawski, C. W. *Angew. Chem., Int. Ed.* **2010**, *49*, 9336−9344.
(7) Yavari, F.; Koratkar, N. *J. Phys. Chem. Lett.* **2012**, *3*, 1746−1753.
(8) Dreyer, D. R.; Park, S.; Bielawski, C. W.; Ruoff, R. S. *Chem. Soc. Rev.* **2010**, *39*, 228−240.
(9) Wu, Z.; Chen, X.; Zhu, S.; Zhou, Z.; Yao, Y.; Quan, W.; Liu, B. *Sens. Actuators, B* **2013**, *178*, 485−493.
(10) Braissant, O. *Mol. Genet. Metab.* **2010**, *100*, S53−S58.
(11) Hummers, W. S.; Offeman, R. E. *J. Am. Chem. Soc.* **1958**, *80* (6), 1339.
(12) Acik, M.; Lee, G.; Mattevi, C.; Pirkle, A.; Wallace, R. M.; Chhowalla, M.; Cho, K.; Chabal, Y. *J. Phys. Chem. C* **2011**, *115*, 19761−19781.
(13) Lu, G.; Ocola, L. E.; Chen, J. *Appl. Phys. Lett.* **2009**, *94*, 083111.
(14) Perrozzi, F.; Prezioso, S.; Donarelli, M.; Bisti, F.; Marco, P. D.; Santucci, S.; Nardone, M.; Treossi, E.; Palermo, V.; Ottaviano, L. *J. Phys. Chem. C* **2013**, *117*, 620−625.
(15) Pei, S.; Cheng, H. M. *Carbon* **2012**, *50* (9), 3210−3228.
(16) Jung, I.; Dikin, D. A.; Piner, R. D.; Ruoff, R. S. *Nano Lett.* **2008**, *8* (12), 4283−4287.
(17) Zhu, Y.; Stoller, M. D.; Cai, W.; Velamakanni, A.; Piner, R. D.; Chen, D.; Ruoff, R. S. *ACS Nano* **2010**, *4* (2), 1227−1233.
(18) Stankovich, S.; Dikin, D. A.; Piner, R. D.; Kohlhaas, K. A.; Kleinhammes, A.; Jia, Y.; Wu, Y.; Nguyen, S. T.; Ruoff, R. S. *Carbon* **2007**, *45*, 1558−1565.
(19) Fowler, J. D.; Allen, M. J.; Tung, V. C.; Yang, Y.; Kaner, R. B.; Weiller, B. H. *ACS Nano* **2009**, *3* (2), 301−306.
(20) Mattevi, C.; Eda, G.; Agnoli, S.; Miller, S.; Mkhoyan, K. A.; Celik, O.; Mastrogiovanni, D.; Granozzi, G.; Garfunkel, E.; Chhowalla, M. *Adv. Funct. Mater.* **2009**, *19*, 2577−2583.
(21) Ren, P. G.; Yan, D. X.; Ji, X.; Chen, T.; Li, Z. M. *Nanotechnology* **2011**, *22*, 055705.
(22) Gao, X.; Jang, J.; Nagase, S. *J. Phys. Chem. C* **2010**, *114*, 832−842.
(23) Shin, H. J.; Kim, K. K.; Benayad, A.; Yoo, S. M.; Park, H. K.; Jung, I. S.; Jin, M. H.; Jeong, H. K.; Kim, J. M.; Choi, J. Y.; Lee, Y. H. *Adv. Funct. Mater.* **2009**, *19*, 1987−1992.
(24) Chua, C. K.; Pumera, M. *J. Mater. Chem. A* **2013**, *1*, 1892−1898.
(25) Yu, K.; Wang, P.; Lu, G.; Chen, K. H.; Bo, Z.; Chen, J. *J. Phys. Chem. Lett.* **2011**, *2*, 537−542.
(26) Cui, S.; Pu, H.; Lu, G.; Wen, Z.; Mattson, E. C.; Hirschmugl, C.; Josifovska, M. G.; Weinert, M.; Chen, J. *ACS Appl. Mater. Interfaces* **2012**, *4*, 4898−4904.
(27) Lu, G.; Yu, K.; Ocola, L. E.; Chen, J. *Chem. Commun.* **2011**, *47*, 7761−7763.
(28) Wu, Z.; Chen, X.; Zhu, S.; Zhou, Z.; Yao, Y.; Quan, W.; Liu, B. *Sens. Actuators, B* **2013**, *178*, 485−493.
(29) Jang, W. K.; Yun, J.; Kim, H.; Lee, Y. S. *Colloid Polym. Sci.* **2013**, *291*, 1095−1103.
(30) Cui, S.; Mao, S.; Wen, Z.; Chang, J.; Zhang, Y.; Chen, J. *Analyst* **2013**, *138*, 2877−2882.
(31) Leenaerts, O.; Partoens, B.; Peeters, F. M. *Phys. Rev. B* **2008**, *77*, 125416.
(32) Tang, S.; Cao, Z. *J. Chem. Phys.* **2011**, *134*, 044710.
(33) Guo, B.; Liu, Q.; Chen, E.; Zhu, H.; Fang, L.; Gong, J. R. *Nano Lett.* **2010**, *10*, 4975−4980.
(34) Mattson, E. C.; Pande, K.; Unger, M.; Cui, S.; Lu, G.; Josifovska, M. G.; Weinert, M.; Chen, J.; Hirschmugl, C. J. *J. Phys. Chem. C* **2013**, *117*, 10698−10707.
(35) Robinson, J. T.; Perkins, F. K.; Snow, E. S.; Wei, Z.; Sheehan, P. E. *Nano Lett.* **2008**, *8* (10), 3137−3140.
(36) Tang, S.; Cao, Z. *J. Phys. Chem. C* **2012**, *116*, 8778−8791.